JOURNAL OF APPLIED ELECTROCHEMISTRY 25 (1995) 364–370

Influence of temperature on electroreduction of anodically formed passive films on lead electrodes in H_2SO_4 solutions
Part II: Electroreduction of PbO layers

F. E. VARELA, L. M. GASSA, J. R. VILCHE*

Instituto de Investigaciones Fisicoquímicas Teóricas y Aplicadas (INIFTA), Facultad de Ciencias Exactas, Universidad Nacional de La Plata, Sucursal 4, C.C. 16, (1900) La Plata, Argentina

Received 12 April 1994; revised 12 June 1994

Combined voltammetry and potentiostatic current transient techniques have been employed to study the electroreduction of anodically formed lead oxide layers, which build up beneath the initially grown $PbSO_4$ crystal, on polycrystalline lead electrodes in concentrated sulphuric acid solution in the 0 to 50° C temperature range. Current transient analysis of the PbO electroreduction performed by using parametric identification procedures and nonlinear fit routines has demonstrated that kinetic data can be mainly interpreted in terms of a progressive nucleation and three-dimensional growth mechanism under charge transfer control, whereas in the initial short time range a process under H^+ ion diffusion control has been detected. The phenomenological explanation of the temperature effect on electrode processes is based on the Arrhenius behaviour of kinetic operational parameters.

1. Introduction

It is a well-known fact that when the lead (Pb) electrode is covered by a $PbSO_4$ layer a basic product PbO is likely to be formed, even in concentrated H_2SO_4 solutions, when the potential is set at sufficiently positive values [1, 2]. This accounts for the $PbSO_4$ layer behaving like a semipermeable membrane, which hinders the diffusion of SO_4^{2-} ions into the pores, causing both an increase in the local Pb(II) ion concentration and a decrease in the H^+ ion concentration at the metal/film interface. Thus, the PbO stability depends on a delicate combination of both pH and potential gradients through the passive film.

Interpretation of the kinetics of PbO electroreduction remains controversial. For instance, it was described qualitatively by Guo [3, 4] as mainly a two-dimensional growth process combined with a relatively slow growth perpendicular to the metal surface, in which nucleation processes can be instantaneous or progressive depending on the applied potential. In previous work [5, 6] we have advanced a quantitative description of both potentiostatic and potentiodynamic results at room temperature on the basis of a progressive nucleation and three-dimensional growth under a charge transfer control process. It has also been pointed out that the electroreduction of PbO layers may be limited on the short time scale by the transport of reacting ions through the anodically formed surface film, this process being controlled by OH^- or H^+ ion diffusion across the $PbSO_4$ membrane [4, 6].

On the other hand, it is interesting to note that photocurrent measurements during the growth of corrosion layers on lead in H_2SO_4 solutions at temperatures in the 25–70° C range have revealed that the thickness of PbO films increases with temperature, so that the film thickness at 70° C was found to be five times greater than that at 25° C [7, 8].

In the present paper potentiostatic current transients corresponding to PbO electroreduction at different temperatures in the 0–50° C range are analysed in order to postulate an appropriate nucleation and growth mechanism to interpret kinetic data. The parametric identification procedure of current transients using nonlinear fit routines allows calculation of the activation energy of kinetic parameters related to the processes involved in the overall reaction pathway.

2. Experimental details

The experimental setup was described in previous publications [5, 9–11]. 'Specpure' lead discs (Johnson Matthey Chemicals Ltd, 0.30 cm^2 apparent area) embedded in PTFE holders were used as working electrodes in 5 M H_2SO_4, under purified nitrogen gas saturation. The electrolyte solution was prepared from analytical grade (p.a. Merck) reagents and triply-distilled water. Measurements were made at five temperatures between 0 and 50° C. Potentials were measured against a Hg/Hg_2SO_4, K_2SO_4(sat.) reference electrode (0.680 V on the NHE scale).

* To whom correspondence should be addressed.

0021-891X

Table 1. Estimated values of E_{exp} from Equation 4 and reported data of E_b^0 [13], solution pH [14] and k_w [15] at different temperatures

$T/°C$	E_b^0/V	$(pH)_s$	$-logK_w$	E_{exp}/V
0	−1.229	−0.842	14.9435	−0.373
25	−1.258	−0.821	13.9965	−0.384
50	−1.287	−0.784	13.2617	−0.387

Prior to the electrochemical experiments the working electrodes were mechanically polished with 600 grade emery paper, thoroughly rinsed in triply-distilled water, and cathodized during $\tau_o = 5$ min at −1.30 V, i.e., in the hydrogen evolution reaction potential range to achieve a reproducible electroreduced lead surface. The dynamic behavior of the electrode was analysed, employing potential sweeps applied at convenience between fixed cathodic ($E_{s,c}$) and anodic ($E_{s,a}$) switching potentials at a scan rate v, and potential steps, usually two covering different preset potential regions. The first potential step ($E_i = E_{s,a} = 0.40$ V) was applied for a set time ($\tau = 30$ s) to modify the anodically formed layer in order to change the total amount of anodic surface products, and the second potential step (E_f) was set sufficiently negative to electroreduce the anodic PbO layer, $-1.04\,V < E_f < -0.90\,V$, but avoiding the electroreduction of $PbSO_4$ crystals. The corresponding current transients were systematically recorded.

3. Results and discussion

3.1. *Voltammetric data*

The voltammograms of lead run at $v = 0.02\,V\,s^{-1}$ between $E_{s,c} = -1.30$ V and $E_{s,a} = 0.40$ V in 5 M H_2SO_4 at different temperatures were shown previously (see, for instance, Fig. 1 in [9]). The magnitude of the PbO electroreduction peak strongly depends on $E_{s,a}$, i.e. for $E_{s,a} \leq -0.40$ V this current peak is not observed, whereas a progressive deactivation of the electrooxidation/electroreduction processes is found as temperature decreases [9]. A qualitative analysis of the potentiodynamic behaviour at room temperature has been given elsewhere [5].

It should be mentioned that both the current density and the voltammetric charge associated with the cathodic peak (C2) related to the electroreduction of PbO layers are slightly dependent on temperature, as was presented in Fig. 1(a) of [9]. Furthermore, when temperature is changed from 45 to 0° C, $E_{p,C2}$ shifts practically 0.022 V more negatively, a value which represents, in principle, a temperature coefficient of about $0.48\,mV\,K^{-1}$. This coefficient cannot be directly related to the shift of the reversible electrode potential. The electroreduction of PbO can be formally represented by

$$PbO + 2H_3O^+ + 2e^- \longrightarrow Pb + 3H_2O \qquad (1a)$$

However, taking into account that the pH of the solution in the interior of a corrosion film containing PbO can be expected to reach a value of 9.34 [12], it appears most appropriate to present the overall reaction as occurring in a basic medium

$$PbO + H_2O + 2e^- \longrightarrow Pb + 2OH^- \qquad (1b)$$

For this reaction the reported reversible potential is $E_b^0 = -1.258$ V (on the Hgse scale) and $-1.163\,mV\,K^{-1}$ is its corresponding isothermal temperature coefficient [13]. The equilibrium potential can be calculated according to

$$E = E_b^0 - (RT/2F)\ln[a_{Pb}a_{OH^-}^2/a_{PbO}a_{H_2O}] \qquad (2a)$$

and assuming solid and water activities as unity, this becomes

$$E = E_b^0 - (RT/F)\ln a_{OH^-} \qquad (2b)$$

where a_{OH^-} corresponds to the activity of OH^- ions at the PbO/metal interface, which can attain a value of $10^{-4.66}$ at 25° C [12]. The PbO layer grows beneath the previously formed $PbSO_4$, which exhibits the characteristics of a membrane with such a pronounced ion selectivity that makes it essentially nonpermeable to SO_4^{2-}, HSO_4^-, and Pb^{2+} ions [5]. Accordingly, an additional diffusion potential should be considered based on either H^+ or OH^- ion concentration difference across the surface film. If $(a_{OH^-})_i$ and $(a_{OH^-})_s$ represent activities of OH^- ions at the PbO/metal interface and in solution, respectively, the diffusion potential is given by

$$\Delta E_d = (RT/F)\ln(a_{OH^-})_i/(a_{OH^-})_s \qquad (3)$$

When the electrode potential of the PbO/Pb interface exposed to the local pH in the interior of the film is being measured experimentally by means of a Hg/Hg_2SO_4 reference electrode, the diffusion potential is included in the measured value. Thus, the externally measured potential becomes

$$E_{exp} = E + \Delta E_d = E_b^0 - (RT/F)\ln(a_{OH^-})_s \qquad (4)$$

which is associated with the PbO/Pb electrode in the external solution pH. Then, to estimate the equilibrium potential at each temperature, it is necessary to know the activity of either OH^- or H^+ ions in the solution. Calculated values of E_{exp} at 0, 25, and 50° C based on data on E_b^0 [13], H^+ ion concentration in 5 M H_2SO_4 measured by Raman spectroscopy [14], and $K_w = (a_{H^+})(a_{OH^-})$ at each temperature [15] are indicated in Table 1. The temperature coefficient is $-0.3\,mV\,K^{-1}$. The temperature-dependent shift of the voltammetric peak potential will be explained in the following section, from results obtained for the PbO electroreduction using the potentiostatic step technique.

3.2. *Electroreduction current transients*

To investigate the kinetics of the electroreduction process by analysis of the corresponding potentiostatic current transients, the PbO layer was allowed to

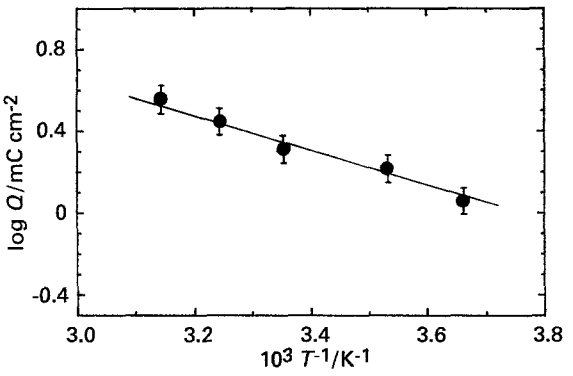

Fig. 1. Dependence of Q, the cathodic charge density on temperature. Data are related to potentiostatic current transients obtained at different temperatures and E_f values within the PbO electroreduction potential range, after potential holding at $E_i = 0.40$ V for $\tau = 30$ s.

grow by including a potential hold for $\tau = 30$ s at $E_{s,a} = 0.40$ V. During this elapsed time, both PbO and $PbSO_4$ layers grew on the lead electrode and, accordingly, a proper separation of the electroreduction processes could be achieved by selecting E_f values. To study the electroreduction mechanism of PbO layers E_f was fixed more positively than -1.04 V [5]. Thus, as temperature increases from 0° C to 45° C a slight activation of the cathodic process as well as higher values of the peak current density j_M at similar times t_M for each E_f was found.

It is noteworthy that the cathodic electroreduction charge (Q), which is independent of E_f, increases with temperature and a linear $\log Q$ against $1/T$ relationship with a slope of approximately -840 decade K (Fig. 1) is obtained. As temperature is increased, the equilibrium potential (E_{exp}) shifts to more negative values (see Table 1) as the formation potential is set at $E_i = E_{s,a} = 0.40$ V in all the cases. Thus, the increase in the PbO electroreduction charge seems to be a consequence of the higher formation overpotential ($E_i - E_{exp}$). Likewise, from the corresponding Q values the thickness (h) of the PbO layer may be estimated and, hence, by considering $M = 223\,g\,mol^{-1}$ and $\rho = 9.53\,g\,cm^{-3}$, h increases from 2.2 nm to 4.4 nm when the temperature is raised from 25 to 45° C. This increase in the PbO layer thickness with temperature agrees with data published by Peter [8] using photoelectrochemical measurements. Values found in that work are higher because the PbO layer was formed over an anodization time $\tau = 50$ min. The formation of PbO arises as a consequence of the local alkalinization at the $Pb/PbSO_4$ interface, so that the local pH change due to the different permeability of the $PbSO_4$ layer determines the PbO layer thickness, attaining a value which is not necessarily constant over the whole electrode surface. Therefore, the value of the PbO layer thickness, estimated from the apparent electroreduction charge, indicates the amount of PbO species previously generated on Pb under the above described experimental conditions only roughly.

More information about the temperature stability

Table 2. Estimated values of K_b and K_a based on thermodynamic data for Reactions 1(a), (b) and 5

T/° C	0	10	25	35	45
$-\log K_b$	16.138	15.822	15.386	15.120	14.870
$-\log K_w$	14.943	14.535	13.996	13.680	13.396
$-\log K_a$	−13.749	−13.247	−12.606	−12.240	−11.922

of the PbO species may be gathered by considering both the PbO electroreduction reaction (Reactions 1(a) or 1(b)) and the direct electroreduction reaction of Pb^{2+} ions

$$Pb^{2+} + 2e^- \longrightarrow Pb \qquad (5)$$

for which a reversible potential $E^0 = -0.8051$ V and a temperature coefficient of $-0.451\,mV\,K^{-1}$ were reported [13]. Thus, under thermodynamic equilibrium conditions, the PbO dissolution reaction without changes in the oxidation state can be expressed by

$$PbO + 2H^+ \rightleftharpoons Pb^{2+} + 2H_2O \qquad (6a)$$

$$PbO + H_2O \rightleftharpoons Pb^{2+} + 2OH^- \qquad (6b)$$

and the corresponding equilibrium constants are

$$K_a = \frac{(a_{Pb^{2+}})(a_{H_2O})}{(a_{PbO})(a_{H^+})^2} \qquad (7b)$$

$$K_b = \frac{(a^{2+}_{Pb})(a_{OH^-})^2}{(a_{PbO})(a_{H_2O})} \qquad (7b)$$

in acid and alkaline aqueous solutions, respectively, so that $K_a = K_b/K_w^2$. From the reversible electrode potentials and temperature coefficients of Reactions 1(b) and 5 it is possible to evaluate K_b

$$K_b = 10^{-7.1766} \exp\left(\frac{-46.838\,kJ\,K^{-1}\,mol^{-1}}{RT}\right) \qquad (8)$$

Values of K_b and K_a calculated for temperatures in the 0 to 45° C range are given in Table 2, where data show that the stability of PbO is only possible in alkaline media and that, due to the variation of K_w, the temperature dependencies of K_b and K_a are opposite, i.e., with increasing temperature K_b is higher whereas K_a is lower.

The cathodic current transients of the PbO layer electroreduction process can be described by the expression [5]

$$j(t) = P_4[1 - \exp(-P_5 t^3)]\exp(-P_5 t^3) + P_6 \exp(-P_7 t) \qquad (9)$$

The first term in Equation 9 corresponds to a progressive nucleation and 3D growth under charge transfer control [16]. Growing nuclei are considered to be right circular cones distributed at random on a planar electrode surface. The second term, which involves a charge density contribution of about 18% of the complete electroreduction of the PbO layer, can be related to an instantaneous nucleation

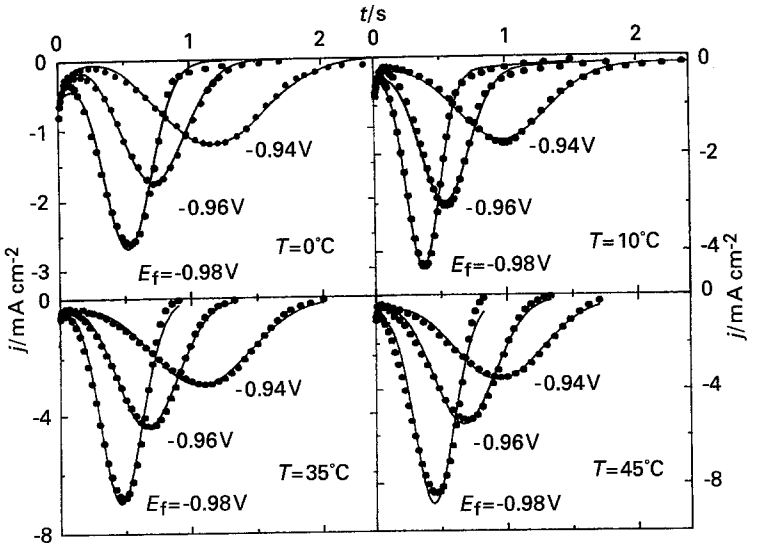

Fig. 2. Comparison of experimental and recorded current transients at different temperatures and E_f in the −0.98 V to −0.94 V potential range after potential holding at $E_i = 0.40$ V for $\tau = 30$ s (●), and calculated data according to Equation 1 (full traces).

and 2D growth under diffusion control [17]. The parameters included in Equation 9 are given by

$$P_4 = zFk_1 \tag{10}$$

$$P_5 = \tfrac{1}{3}\pi M^2 k_2^2 A \rho^{-2} \tag{11}$$

$$P_6 = q_{\text{mon}} \pi K_h D_h N_0' \tag{12}$$

$$P_7 = \pi K_h D_h N_0' = P_6/q_{\text{mon}} \tag{13}$$

where k_1 and k_2 denote the rate constants describing crystal growth perpendicular and parallel to the plane surface electrode, respectively, A is the nucleation rate constant, $K_h = (8\pi c_h M \rho^{-1})^{1/2}$, q_{mon} the monolayer charge density, N_0' the number of active centres, ρ the density of the layer, M the PbO molecular weight, and D_h the diffusion coefficient of the species of concentration c_h.

Figure 2 illustrates the good agreement between experimental and calculated data from Equation 9. The decrease in temperature promotes, in principle, a deactivation of the PbO electroreduction process, although this deactivation is smaller than that reported for the $PbSO_4$ electroreduction [9]. At constant temperature, the optimal set of fit parameters can be calculated and the corresponding potential dependencies of P_4 and P_5 are shown in Fig. 3 in the form of $\log P_h$ ($h = 4, 5$) against E_f plots.

The exact expression for the kinetic constants (both k_1 and k_2) in terms of the absolute rate theory is given by [18]

$$k = \tau^* \left(\frac{kT}{h}\right) \exp\left(\frac{\Delta S^{0*}}{R}\right) \exp\left(-\frac{\Delta H^{0*}}{RT}\right) \times \exp\left(-\frac{\beta z F}{RT}\eta\right) \exp\left(-\frac{\beta z F}{RT} E_{\text{rev}}\right) \tag{14}$$

where τ^* is the transmission coefficient (which can be considered approximately unity [18]), $\Delta G^{0*} = \Delta H^{0*} - T\Delta S^{0*}$ the standard free energy of activation for ordinary chemical reaction (not electrochemical), E_{rev} the reversible electrode potential of the electrochemical process in question, and η the overpotential. All other symbols have their usual meaning. From Equations 10 and 14 it follows that the slope of either $\log P_4$ against E_f or $\log P_4$ against η plots at each temperature allows estimation of the value of β_1. Data given in Table 3 indicate that $\beta_1 = 0.584 \pm 0.003$ for the whole temperature range covered in this work. Furthermore, Table 3 reveals that the slopes of $\log P_5$ against E_f plots depicted in Fig. 3(b) are about to three times those of $\log P_4$

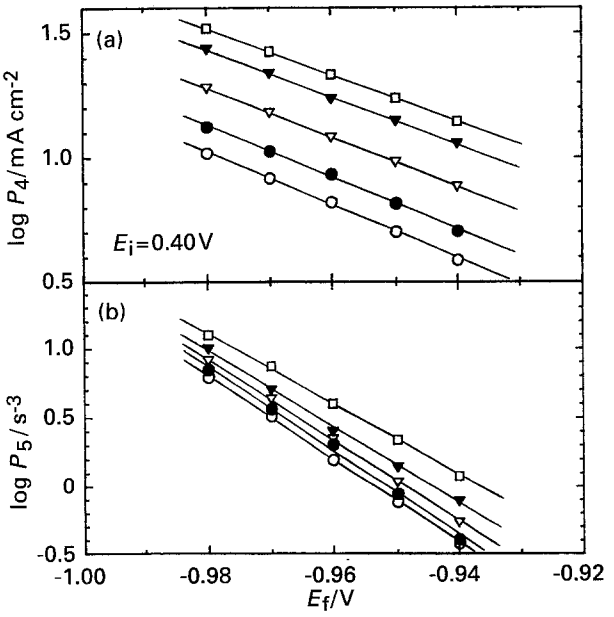

Fig. 3. Dependence of (a) P_4 and (b) P_5 on E_f at different T in the 0° C ≤ T ≤ 45° C range. Data related to current transients depicted in Fig. 2. T: (□) 45, (▼) 35, (▽) 25, (●) 10 and (○) 0° C.

Table 3. Calculated values of the potential dependencies of kinetic parameters at different temperatures from Fig. 3. The β_1 values were estimated from $\partial \log P_4/\partial E_f$ and Equation 14

T/° C	$\partial \log P_4/\partial E_f$ /decade mV^{-1}	β_1	$\partial \log P_5/\partial E_f$ /decade mV^{-1}
0	−10.725	0.581	−31.339
10	−10.455	0.587	−31.148
25	−9.906	0.586	−29.588
35	−9.496	0.580	−28.101
45	−9.315	0.588	−26.830

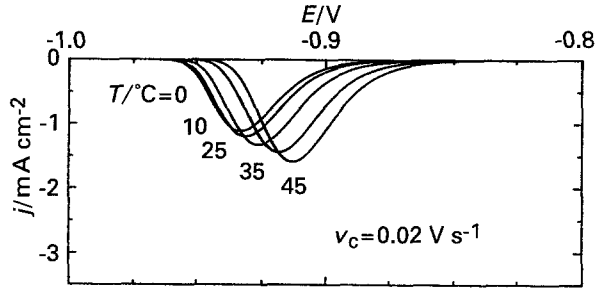

Fig. 4. Simulated cathodic voltammograms corresponding to the electroreduction of the PbO layer formed at $E_i = 0.40$ V for $\tau = 30$ s according to the potential dependencies of parameters P_4 and P_5 depicted in Fig. 3.

against E_f plots at each temperature. This means $(\partial \log P_5/\partial E_f)_T = 3(\partial \log P_4/\partial E_f)_T$ [5]. Taking into account that P_5 includes both k_2 and A, which are potential dependent, it is impossible to estimate the value of β_2.

In previous work [6], it was demonstrated that the voltammetric profile related to the PbO electroreduction can be simulated from knowledge of the potential dependencies of parameters P_4 and P_5 (Fig. 3), and that both potentiodynamic and potentiostatic PbO electroreduction follow the same nucleation and 3D growth under charge transfer control. A description of the computer simulation has been given elsewhere [9, 19]. Simulated cathodic voltammograms corresponding to the electroreduction of the PbO layer formed at $E_i = 0.40$ V for a $\tau = 30$ s are presented in Fig. 4, where the peak potential $E_{p,C2}$ is shifted 21 mV to more positive values when the temperature increases from 0 to 45° C. This corresponds to a temperature coefficient of about 0.47 mV K^{-1}, a value close to that found from the experimental voltammograms run at different temperatures. Fletcher *et al.* [20] have shown that when a voltammetric current peak is related to a nucleation and growth controlled reaction, the peak potential depends on the kinetic parameter of the process. Thus, it is clear that the

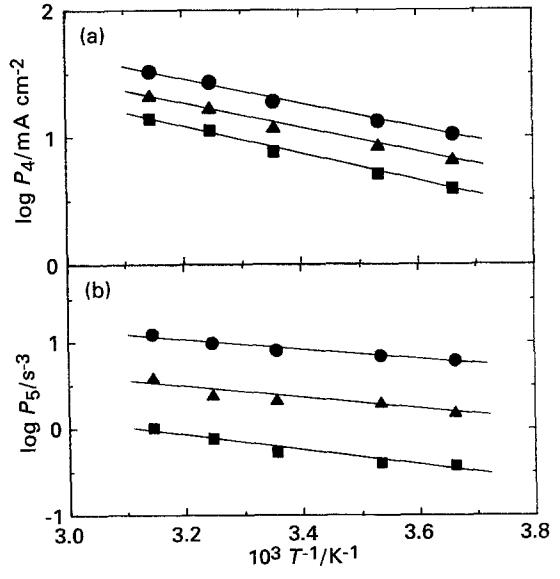

Fig. 5. Dependence of (a) P_4 and (b) P_5 on T at different E_f in the $-0.980\text{ V} \leq E_f \leq -0.940$ V range. Data related to current transients depicted in Fig. 2. E_f: (●) −0.980, (▲) −0.960 and (■) −0.940 V.

Table 4. Apparent activation enthalpies estimated from Arrhenius plots shown in Fig. 5. The values of ΔH^*_Q were calculated from Equation 17(a)

E_f/V	$\Delta H^*_{P_4}$ /kJ mol^{-1}	$\Delta H^*_{P_5}$ /kJ mol^{-1}	ΔH^*_Q /kJ mol^{-1}
−0.980	18.934	10.941	15.287
−0.970	19.075	12.024	15.067
−0.960	19.162	12.606	14.960
−0.950	20.260	15.597	15.061
−0.940	21.129	16.485	15.634

shift of the peak potential in the voltammograms corresponding to the potentiodynamic electroreduction of PbO layers can be attributed to an inversion of the rate constants describing both crystal growth (k_1 and k_2) and nucleation (A) with temperature. This can also be deduced from results presented in Fig. 3, so that with increasing temperature the electroreduction process should be faster and should occur at more positive potentials, the latter implying lower cathodic overpotentials.

Rate constants fit an Arrhenius-type behaviour,

$$k = Z \exp\left(-\frac{\Delta H^*}{RT}\right) \qquad (15)$$

where Z denotes the frequency factor and ΔH^* the apparent activation enthalpy. The activation enthalpy of the PbO layer electroreduction under charge transfer control can be estimated from the straight lines of $\log P_h$ ($h = 4, 5$) against $1/T$ Arrhenius plots (Fig. 5) whose slopes yield the corresponding values of ΔH^* which, at different E_f, are given in Table 4. These results suggest that the thermal increase in the crystal growth perpendicular to the plane surface electrode is about twice that in the parallel direction. Comparing Equations 14 and 15, and neglecting the temperature effect involved in the linear term (kT/h), it becomes clear that the evaluation of ΔH^* from the slope of a $\log k$ against T^{-1} plot includes two contributions according to $\Delta H^* = \Delta H^{0*} - \beta \Delta H^0$, where ΔH^{0*} is related to the ordinary chemical reaction and ΔH^0 to the reversible electrochemical reaction. Accordingly, ΔH^0 increases and ΔH^* diminishes with the electroreduction potential as observed in Table 4. Then, ΔH^{0*} can be estimated from ΔH^* after introducing theoretical values of ΔH^0, which could not be calculated very precisely [18]. However, for the same overall reaction (in this case, both k_1 and k_2 correspond to the electroreduction of PbO to Pb), the differences in true activation energies and the ratio of true frequency factors could be deduced. According to Equation 11 the parameter P_5 takes into account two temperature-dependent terms, which follow an Arrhenius-type behaviour A, the nucleation rate constant, and k_2, the rate constant describing crystal growth parallel to the plane surface electrode. Under these circumstances it is practically impossible to calculate the value of ΔH^* for k_2.

As the first term in Equation 9 comprises the

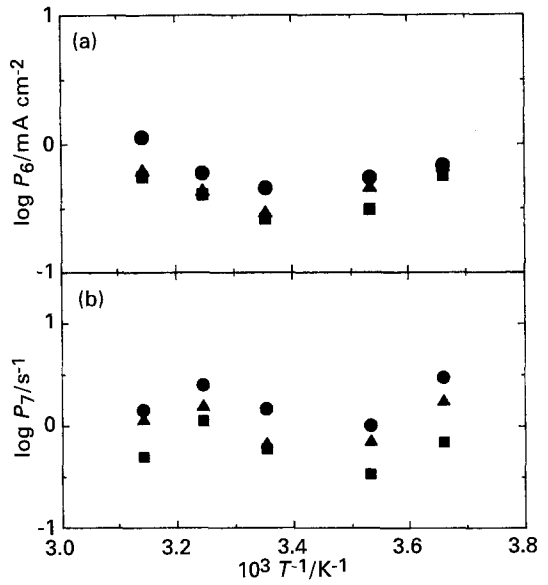

Fig. 6. Dependence of (a) P_6 and (b) P_7 on T at different E_f in the $-0.980\,V \leq E_f \leq -0.940\,V$. Data related to current transients depicted in Fig. 2. E_f: (●) −0.980, (▲) −0.960 and (■) −0.940 V.

main current contribution, the cathodic charge involved in the electroreduction of PbO layers can be approximated by [5]

$$Q \approx 0.18 P_4 P_5^{-1/3} \tag{16}$$

and, hence,

$$(\partial \log Q/\partial T^{-1}) \approx (\partial \log P_4/\partial T^{-1}) - \tfrac{1}{3}(\partial \log P_5/\partial T^{-1}) \tag{17a}$$

Taking into account Equations 10 and 11, Expression 17(a) can be rewritten in the form

$$(\partial \log Q/\partial T^{-1}) \approx (\partial \log k_1/\partial T^{-1}) - \tfrac{1}{3}(\partial \log k_2^2 A/\partial T^{-1}) \tag{17b}$$

Introducing results obtained from the slopes of $\log P_h$ ($h = 4, 5$) against E_f plots presented in Table 4 as $\Delta H^*_{P_4}$ and $\Delta H^*_{P_5}$, into Equation 17(a) theoretical values of ΔH^*_Q ($\partial \log Q/\partial T^{-1}$) indicated in Table 4 are obtained. The calculated temperature dependence of the cathodic charge corresponding to PbO electroreduction, is close to the value 16.0 kJ mol^{-1} resulting from the experimental data presented in Fig. 1.

In relation to the influence of temperature on the diffusional process characterized by P_6 and P_7, it is important to note that q_{mon} calculated from Equation 5 remains at a practically constant value, $q_{mon} = 0.46 \pm 0.05$ mC cm^{-2}, at least in the temperature range covered in this work. In previous work [6], it was suggested that the initial (short time range) current decay during the PbO electroreduction can be associated with the electroreduction of Pb(II) ions controlled by the diffusion of H^+ from the outer $PbSO_4$ layer to the inner portion of the passive film. From the activity of H^+ $a_{H^+} = 10^{-9.34}$, which was estimated for the generation of a stable PbO layer [12, 21], and assuming, for the sake of comparison, a value of $N'_0 \approx 10^{10}$ cm^{-2}, according to Equation 5 a mean value of D_h at 25° C close to 6×10^{-7} cm^2 s^{-1} can be calculated in agreement with that expected for a diffusion process taking place in the pores of the passive film. Finally, the fact that the activation energy cannot be clearly evaluated from the Arrhenius plot suggests that it has a very small value, which is consequently hidden within the experimental scatter (Fig. 5).

4. Conclusions

Kinetic data analysis suggests that the nucleation and growth mechanism developed to interpret the electroreduction of PbO layers formed on Pb in H_2SO_4 solutions at room temperature can be successfully used in the 0 to 45° C temperature range.

The electroreduction of the PbO layer, which builds up beneath the initially grown $PbSO_4$ layer, consists of two current contributions. One term is associated with an instantaneous nucleation and 2D growth under diffusion control, which can be related to the electroreduction of Pb(II) ions controlled by the diffusion of H^+ to the inner portion of the complex passive film structure. The second term, which constitutes the main current contribution, can be assigned to a progressive nucleation and 3D growth mechanism under charge transfer control. The latter accounts for kinetic data on the electroreduction of the PbO layer itself, which constitutes the inner portion of the passive film structure.

The effect of decreasing temperature promotes deactivation of electroreduction of PbO layers. The temperature dependence of the overall kinetics is interpreted on the basis of Arrhenius-type behaviour observed for the different kinetic parameters involved in the whole reaction mechanism.

Acknowledgement

This research project was financially supported by the Consejo Nacional de Investigaciones Científicas y Técnicas, the Comisión de Investigaciones Científicas de la Provincia de Buenos Aires, and the Fundación Antorchas. Part of the equipment used in the present work was provided by the DAAD and the Alexander von Humboldt-Stiftung.

References

[1] D. Pavlov, *Electrochim. Acta* **23** (1978) 845.
[2] D. Pavlov and N. Iordanov, *J. Electrochem. Soc.* **117** (1970) 1103.
[3] Y. Guo, *J. Electroanal. Chem.* **317** (1991) 229.
[4] *Idem, Electrochim. Acta* **37** (1992) 495.
[5] F. E. Varela, L. M. Gassa and J. R. Vilche, *ibid.* **37** (1992) 1119.
[6] F. E. Varela, E. N. Codaro and J. R. Vilche, *Electrochim. Acta*, submitted.
[7] L. M. Peter, *Ber. Bunsenges. Phys. Chem.* **91** (1987) 419.
[8] J. S. Buchman and L. M. Peter, *Electrochim. Acta* **33** (1988) 127.
[9] F. E. Varela, L. M. Gassa and J. R. Vilche, *J. Appl. Electrochem.*, submitted.
[10] *Idem, J. Electroanal. Chem.* **353** (1993) 147.

[11] F. E. Varela, M. E. Vela, J. R. Vilche and A. J. Arvia, *Electrochim. Acta* **38** (1993) 1513.
[12] P. Ruetschi, *J. Electrochem. Soc.* **120** (1973) 331.
[13] Z. Galus, in 'Standard Potentials in Aqueous Solution' (edited by A. J. Bard, R. Parsons and J. Jordan), Marcel Dekker, New York (1985) pp. 220–235.
[14] W. J. Hamer (ed.), 'The Structure of Electrolytic Solutions', John Wiley & Sons, New York (1959) pp. 48–55.
[15] 'Handbook of Chemistry and Physics', 67th ed., CRC Press, Boca Raton, Florida (1987).
[16] R. D. Armstrong, M. Fleischmann and H. R. Thirsk, *J. Electroanal. Chem.* **11** (1966) 208.
[17] R. D. Armstrong and J. A. Harrison, *J. Electrochem. Soc.* **116** (1969) 328.
[18] B. E. Conway, in 'Theory and Principles of Electrode Processes' (edited by B. Crawford, W. D. McElroy and C. C. Price) The Ronald Press Company, New York (1965) pp. 92–109.
[19] F. E. Varela, J. R. Vilche and A. J. Arvia, *Electrochim. Acta.* **39** (1994) 401.
[20] S. Fletcher and A. Smith, *Can. J. Chem.* **56** (1978) 606.
[21] Y. Guo, *J. Electrochem. Soc.* **139** (1992) 2114.